

Synthesis and molecular docking studies of pyrazolo-oxazole derivatives as potential inhibitors of *P. gingivalis* heme-binding protein

Nagendra Kumar Pandey^a, Ashok Kumar^a, Rashmi Sharma^b, Deepika Geedkar^a and Pratibha Sharma^{a*}

^aSchool of Chemical Sciences, Devi Ahilya Vishwavidyalaya, Indore (M.P.), India

^bShri Vaishnav Vidyapeeth Vishwavidyalaya, Indore (M.P.), India

CHRONICLE

Article history:

Received October 3, 2024

Received in revised form

November 4, 2024

Accepted February 25, 2025

Available online

February 25, 2025

Keywords:

Heterocyclic Scaffolds

Pyrazolo-oxazoles

Molecular Docking

Drug Discovery

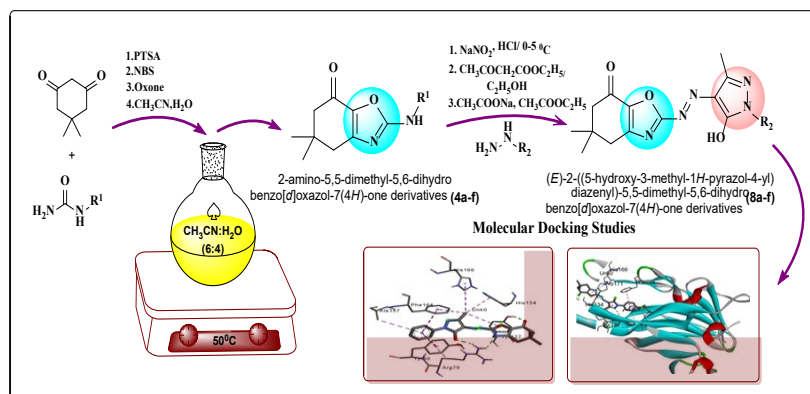
P. gingivalis

Heme-Binding Protein

ABSTRACT

The present paper elicits the studies on synthesis and potential pharmacological applications of pyrazolo-oxazole heterocyclic scaffolds. The synthesized compounds were characterized by different spectroanalytical tools including ¹H NMR, ¹³C NMR, and FTIR techniques, followed by molecular docking-based biological interaction studies. Synthesized pyrazolo-oxazoles (**8a-f**) were docked against the heme-binding protein of *P. gingivalis*, an oral pathogen, responsible for a number of diseases. Among the synthesized heterocycles, compounds (**8e**) and (**8f**) showed better docking scores compared to the marketed drugs and thus are of great interest as lead compounds in developing treatment profiling to combat *P. gingivalis*-borne diseases.

© 2025 by the authors; licensee Growing Science, Canada.



Graphical Abstract

1. Introduction

In recent times, the majority of pharmaceutically active chemical compounds possess heterocyclic skeletons in their core armamentarium, highlighting their importance in the drug discovery domain.¹⁻¹¹ These heterocycles can be traced in a number of well-established drugs belonging to different categories with diverse therapeutic activities. A number of synthetic as well as naturally occurring heterocycles play an important role in medical research^{12,13} and endorse their presence as hormones, antibiotics, vitamins¹⁴, etc. In particular, nitrogen-containing heterocyclic compounds such as quinoline, indoles, pyrroles, oxazoles, and pyrrolidines play a significant role in medicinal chemistry.^{17,18}

* Corresponding author

E-mail address profpratibhasharma@gmail.com (P. Sharma)

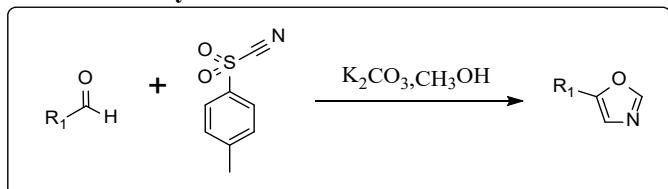
© 2025 by the authors; licensee Growing Science, Canada

doi: 10.5267/j.ccl.2025.2.007

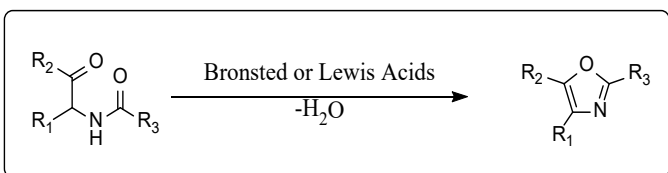
A number of synthetic methods for constructing oxygen/nitrogen-containing heterocyclic derivatives have appeared in the existing literature protocols.¹⁹⁻²³ The literature²⁴ emphasizes the effectiveness and adaptability of the Van Leusen oxazole synthesis, which involves the reaction of Tos MIC (tosyl methyl isocyanide) with aldehydes or ketones. The technique is commended for its capability to produce oxazole nucleus with considerable functional group tolerance and under a variety of substrate conditions. Likewise, pyrazole and its derivatives are considered a pharmacologically important active scaffold that possesses almost all types of pharmacological activities. The presence of this nucleus in pharmacological agents of diverse therapeutic categories such as celecoxib, a potent anti-inflammatory, the antipsychotic CDPPB, the anti-obesity drug rimonabant, difenamizole, an analgesic, betazole, a H₂-receptor agonist and the antidepressant agent fezolamide have proved the pharmacological potential of the pyrazole moiety. Owing to this diversity in the biological field, this nucleus has attracted the attention of many researchers to study its skeleton chemically and biologically. Moreover, one-pot multicomponent synthesis has emerged as the popular and eco-friendly protocol for synthesizing heterocycles. Such methodology has been proven considerably fruitful in diversified domains, viz., drug discovery, pharmaceuticals, combinatorial chemistry, and catalysis. Nevertheless, the multicomponent reaction strategies leading to generating fused oxazolo-pyrazole framework have risen dramatically in the last two decades. The fused heterocycles are crucial in medicinal chemistry due to their ability to create diverse and complex molecular structures. Also, structural motifs derived from two linked heterocycles are important in medicinal chemistry because they allow for the creation of molecules with enhanced biological activity and diverse properties by combining the unique characteristics of each heterocyclic ring, often leading to improved potency, selectivity, and drug-like properties compared to single heterocyclic compounds; this is particularly valuable for designing new drugs with complex therapeutic targets. Furthermore, synthesized compounds are subjected to molecular interactions with biological targets, leading to the discovery of new molecules that may hold promise for therapeutic ailments related to *P. gingivalis*. The chemical interactions that may guide the optimization of these drugs to maximize their efficacy while reducing their toxicity have been identified by molecular docking studies. Hence, keeping in view the aforementioned importance of these heterocycles, it was thought worthwhile to design and develop a series of heterocyclic compounds embracing azo functionality flanked between oxazolo-pyrazole framework. An overview of literature protocols is depicted in scheme-1, whereas, strategy to synthesize a library of substituted 2-amino-5,5-dimethyl-5,6-dihydro-1,3-benzoxazol-7(4H)-one (**4a-f**) and (E)-2-((5-hydroxy-3-methyl-1H-pyrazol-4-yl)diazonyl)-5-methyl-5,6-dihydrobenzo[d]oxazol-7(4H)-one (**8a-f**) developed in our laboratory, is given in **Scheme 2**.

PREVIOUS APPROACH

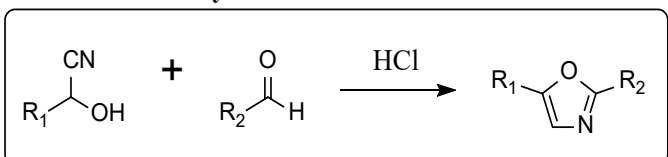
A. Van-leusen synthesis



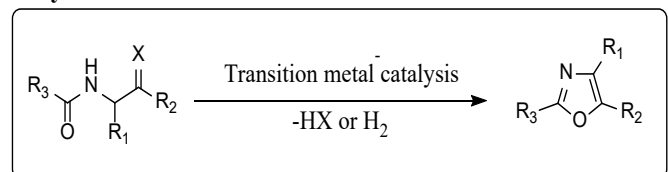
B. Robison-Gebriel condensation



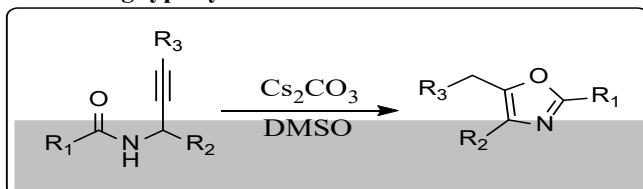
C. Fisher oxazole synthesis



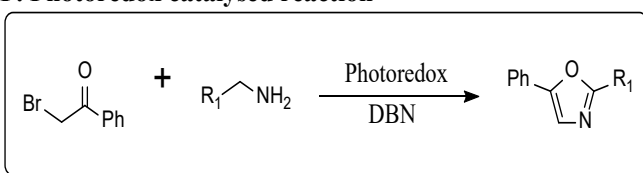
D. Cyclisation of enamides



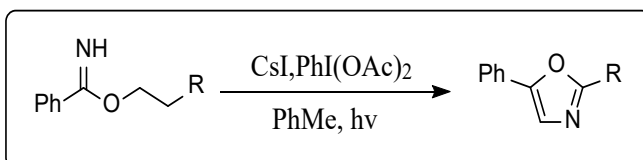
E. 5-exo dig type cyclisation



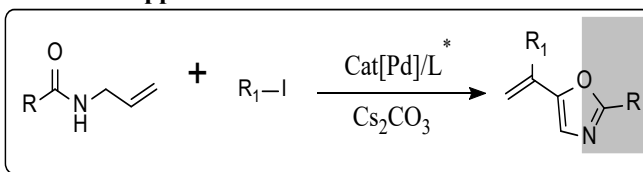
F. Photoredox catalysed reaction



H. Double HAT mechanism

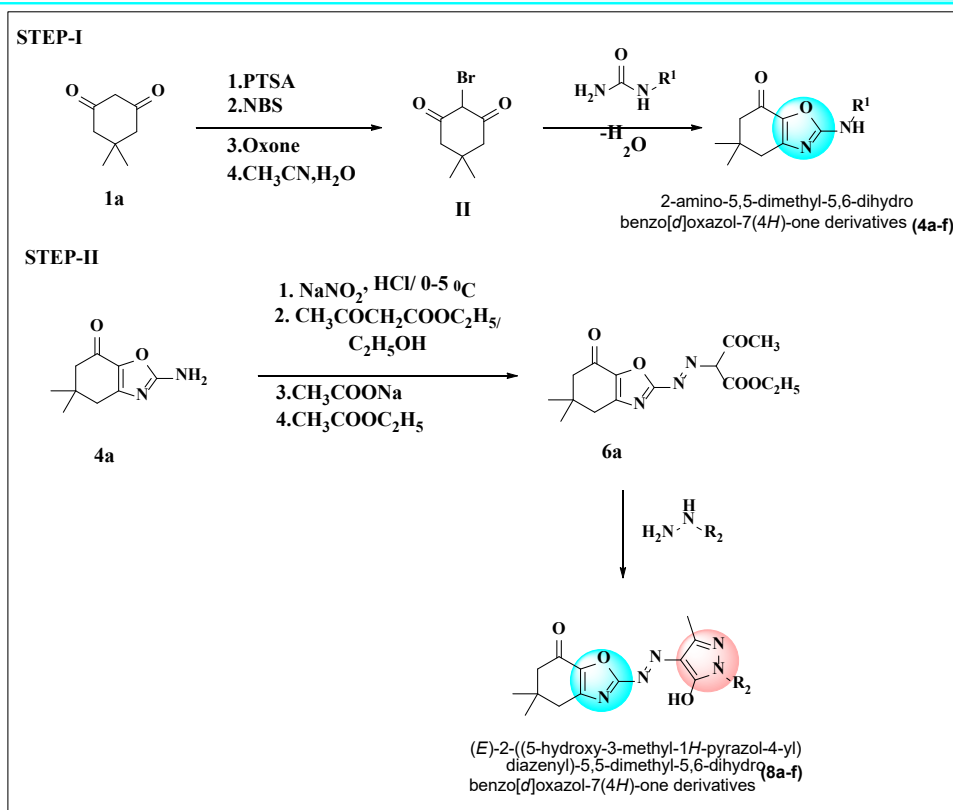


H. Allene's approach to oxazoline



Scheme 1. An overview of literature protocols

OUR APPROACH



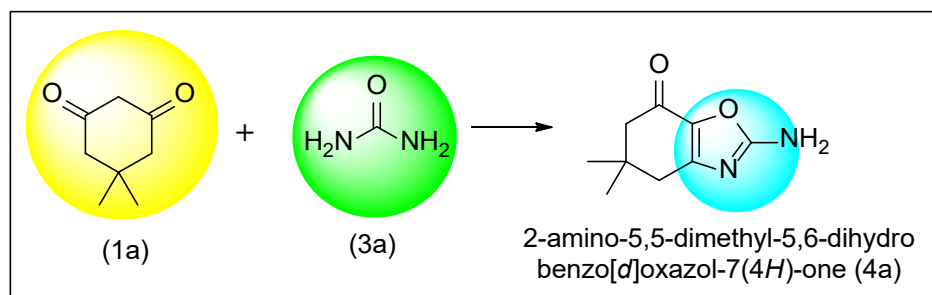
Scheme 2.

2. Results and Discussion

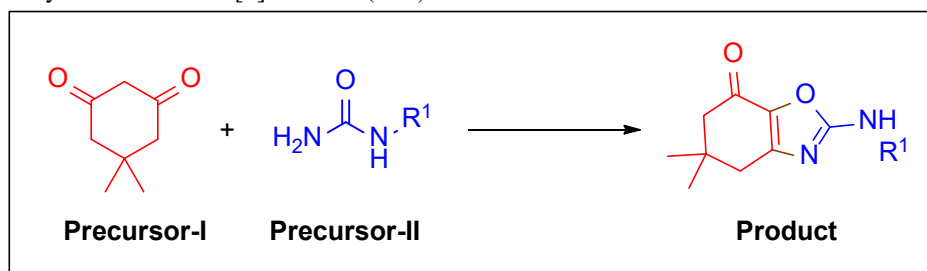
2.1. Reaction Conditions Optimization for the Synthesis of Benzo[d]oxazoles

To synthesize fused oxazole, we first optimized the reaction using urea derivatives and dimedone as model reactants. Dimedone was initially converted to 2-bromocyclohexan-1,3-one using the brominating reagent NBS (N-Bromosuccinimide) (1.3 mmol; **Table 1**, entry 12). For this *in situ* transformation, we investigated various organic solvents, including binary mixtures of both aprotic and protic solvents such as CH₃CN (3.92 D), THF (1.75 D), CH₃OH (1.5 D), and CH₂Cl₂ (1.60 D). Among these, the acetonitrile and water mixture in a 6:4 v/v ratio was found to be the most effective (**Table 1**, entry 15). Organic aprotic solvents like acetonitrile (3.92 D) facilitate the diffusion of charged species in solution, making them ideal for sustainable routes and green chemistry applications. The reaction becomes more experimentally efficient when the aqueous fraction of the acetonitrile-water mixture is increased.

To further enhance the reaction yield, the process was carried out at various temperatures. The optimal yield was achieved when the reaction between 2-bromocyclohexanone (III) and urea derivatives (3a–f) was conducted at 50 °C (Table 1, entry 15). Literature reports difficulties in regulating the amount of O₂ gas as an oxidant. It has been realized that molecular oxygen can be highly explosive and requires high pressure to be effective as an oxidant. Moreover, oxidants based on transition metals are often associated with environmental and health hazards. Therefore, we performed reactions in alternative oxidants, such as oxone, CAN (Ceric ammonium nitrate), m-CPBA (m-Chloroperoxybenzoic acid), and 70% TBHP (tert-Butyl hydroperoxide), however, out of these, oxone showed the best performance (Table 1, entry 9). To address these issues, we selected oxone as a green oxidant under the following ideal conditions: 50 °C, NBS (1.3 mmol), PTSA (p-toluene sulfonic acid) (1.5 mmol), acetonitrile-water (10 mL, 6:4 v/v), and oxone (1.3 mmol) (Table 1). Scheme 3 provides a schematic representation of the synthetic pathway. The use of oxone also facilitates the *in situ* formation of 2-bromocyclohexan-1,3-one.²⁶

Table 1. Optimization of the reaction conditions for the preparation of 2-amino-5,5-dimethyl-5,6-dihydro-1,3-benzoxazol-7(4*H*)-one (**4a**)

Entry	NBS (mmol)	PTSA (mmol)	External Oxidant	Solvent (v/v)	Temperature (°C)	Yield (%)
1.	1	1	m-CPBA	CH ₃ CN:H ₂ O (7:3)	Reflux	Trace
2.	1	1	m-CPBA	CH ₃ OH:H ₂ O (7:3)	Reflux	n.r.
3.	1	1	m-CPBA	THF:H ₂ O (7:3)	Reflux	n.r.
4.	1	1	60%TBHP	CH ₃ OH:H ₂ O (7:3)	Reflux	n.r.
5.	1	1	60%TBHP	CH ₃ CN:H ₂ O (7:3)	Reflux	n.r.
6.	1	1	60%TBHP	CH ₃ CN:H ₂ O (7:3)	Reflux	n.r.
7.	1	1	CAN	CH ₃ CN:H ₂ O (7:3)	Reflux	36
8.	1	1	CAN	CH ₃ OH:H ₂ O (7:3)	Reflux	35
9.	1	1	CAN	THF:H ₂ O (7:3)	Reflux	30
10.	1	1	Oxone	CH ₃ CN:H ₂ O (8:2)	Reflux	45
11.	1	1	Oxone	CH ₃ OH:H ₂ O (7:3)	Reflux	trace
12.	1	1	Oxone	THF:H ₂ O (7:3)	Reflux	n.r
13.	1.3	1.5	Oxone	CH ₃ CN:H ₂ O (7:3)	Reflux	49
14.	1.3	1.5	Oxone	CH ₃ CN:H ₂ O (7:3)	60	73
15.	1.3	1.5	Oxone	CH ₃ CN:H ₂ O (7:3)	50	85
16.	1.3	1.5	Oxone	CH ₃ CN:H ₂ O(6:4)	50	92
17.	1.3	1.5	Oxone	CH ₃ CN:H ₂ O (5:5)	40	85

Table 2. Library of synthesized Benzo[*d*]oxazoles (4a-f)

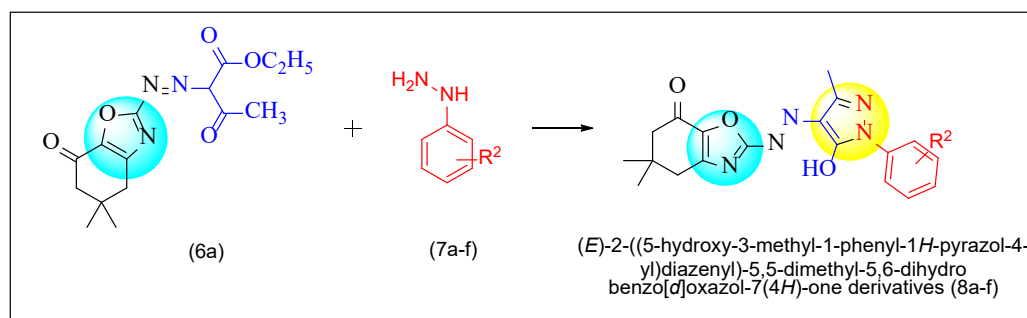
Entry	Precursor-I	Precursor-II	Product	Time (min.)	Yield (%)
1.	1a	3a	4a	50	92
2.	1a	3b	4b	50	87
3.	1a	3c	4c	50	86
4.	1a	3d	4d	50	84
5.	1a	3e	4e	50	85
6.	1a	3f	4f	50	88

These encouraging results confirm that the current protocol is a flexible, economical, and practical method for the synthesis of fused-oxazole derivatives (4a-f). Additionally, a cascade reaction (**Scheme 3**) was employed to synthesize a series of fused-oxazoles (4a-f) using substituted urea and dimedone as precursors under the same optimized reaction conditions. This method produced the desired products in yields ranging from modest to excellent, which is notable (**Table 2**). However, slightly lower yields were observed for substituted derivatives, which can be attributed to the electron-withdrawing nature of certain substituents.

2.2. Optimization of Reaction Conditions for the Synthesis of Pyrazolo-Oxazoles

A series of pyrazolo-oxazole compounds were synthesized under optimized reaction conditions. To evaluate the feasibility of the reaction, optimization studies were conducted concerning different solvents, temperature, and reaction time. To assess the effect of various solvents, the reaction was carried out in dichloromethane, dimethylformamide (DMF), methanol, water, and under solvent-free conditions. These optimizations showed that polar protic solvents such as dichloromethane, DMF, and water resulted in very low product yields. Methanol gave noticeable yields, but solvent-free conditions led to the highest yields (Table 3, entry 7). Based on these results, the reaction was conducted under solvent-free conditions. Similarly, optimization studies of temperature and reaction time determined that a reaction time of 2 hours at 50°C was optimal for producing the final product. Increasing the temperature beyond 50°C resulted in decreased product yields. Regular monitoring of the reaction through TLC studies revealed that higher temperatures consistently led to lower yields for all the optimized compounds. An overview of the optimization studies is summarized in Table 3.

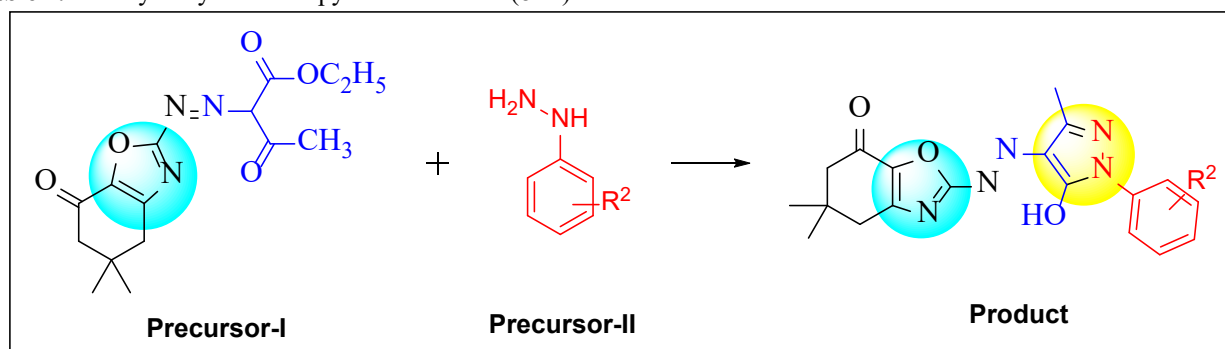
Table 3. Optimization of the reaction conditions for the preparation of pyrazolo-oxazole (8a-f).



Entry	Aza compound	R ₂	Product	Solvent	Time	Temperature	Yield (%)
1.	6a	7a	8a	THF	2 hrs	70	n.r
2.	6a	7b	8b	DMF	2 hrs	50	n.r
3.	6a	7b	8b	CH ₂ CL ₂	2 hrs	60	trace
4.	6a	7a	8a	H ₂ O	2 hrs	80	trace
5.	6a	7a	8a	CH ₃ OH	2 hrs	40	63
6.	6a	7a	8a	CH ₃ OH	2hrs	50	70
7.	6a	7b	8b	Solvent free	2 hrs	60	92
8.	6a	7a	8a	Solvent free	2hrs	50	85
9.	6a	7b	8b	Solvent free	1.5hrs	60	74

Compounds with electron-donating groups showed an increase in product yield, while those with electron-withdrawing substituents exhibited a decrease. A summary of the optimization studies is provided in Table 3 and Table 4. Subsequently, a library of six distinct fused oxazole-linked pyrazole compounds was synthesized under the optimized conditions (Table 4).

Table 4. Library of synthesized pyrazolo-oxazole (8a-f)



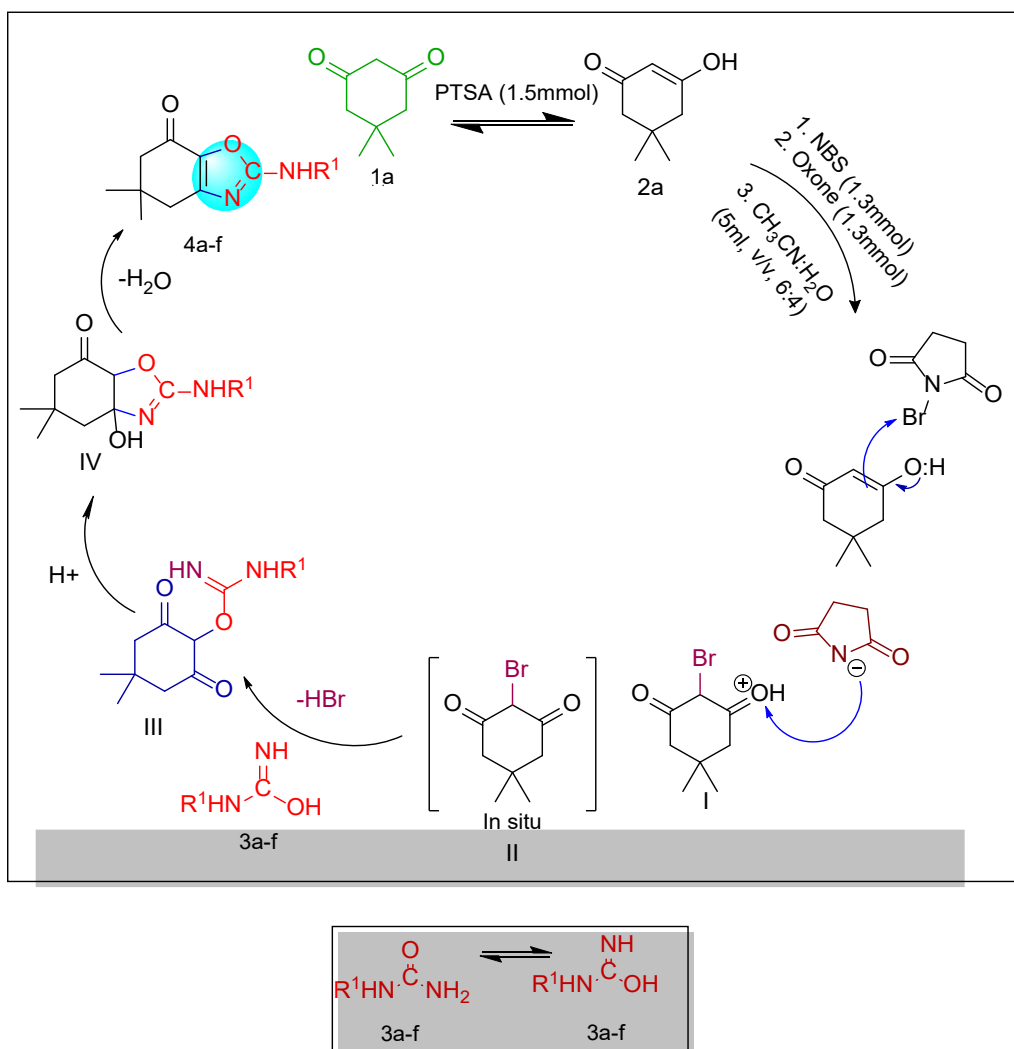
Entry	Precursor-I	Precursor-II	Product	Time	Yield (%)
1.	4a	7a	8a	2 hrs	90
2.	4a	7b	8b	2 hrs	87
3.	4a	7c	8c	2 hrs	86
4.	4a	7d	8d	2 hrs	84
5.	4a	7e	8e	2 hrs	85
6.	4a	7f	8f	2 hrs	88

2.3. Plausible Reaction Mechanism

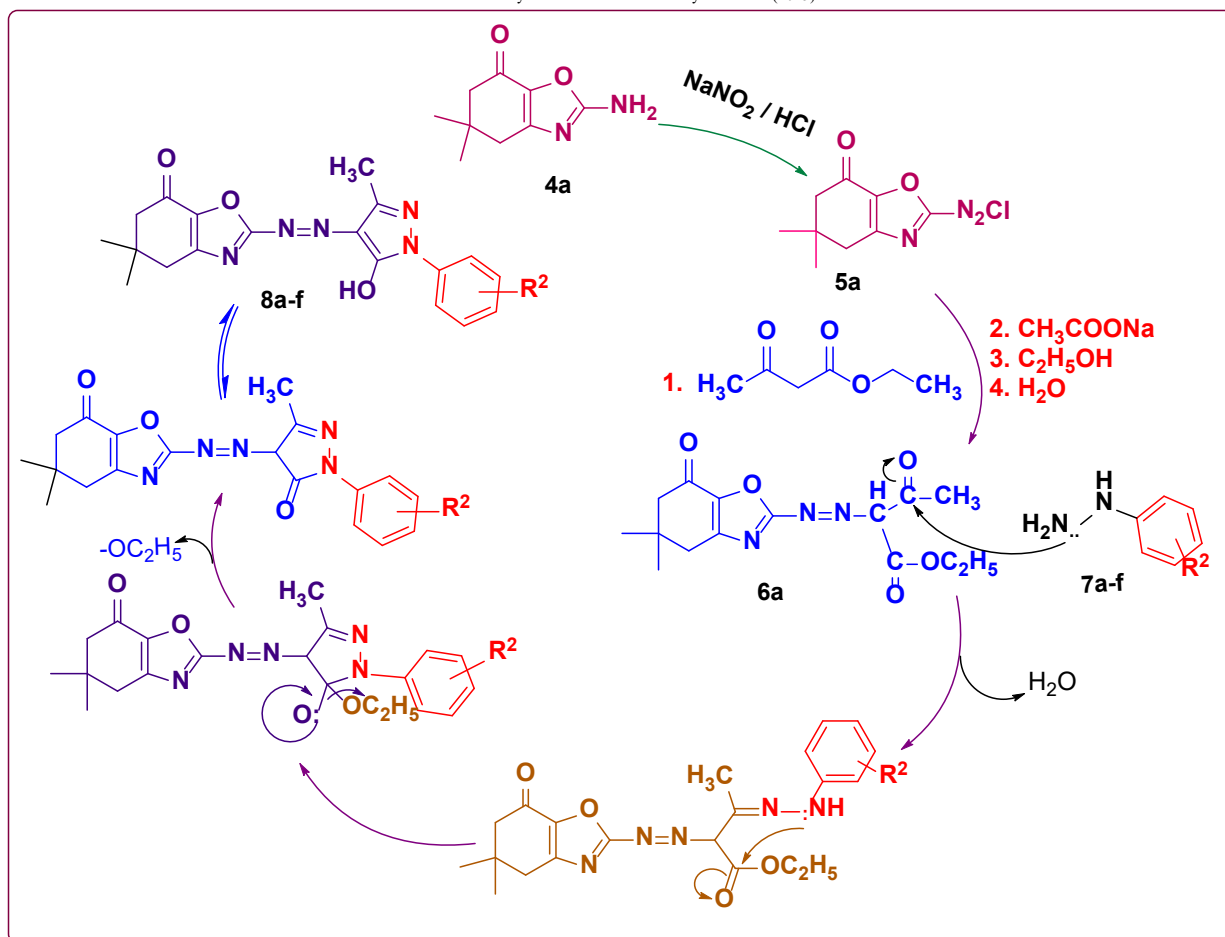
In Scheme 3, the reaction begins when PTSA is introduced to reactant **1a**, establishing an acidic environment that triggers keto-enol tautomerism. This process involves proton exchange between the carbonyl oxygen and the α -carbon, leading to the formation of 3-hydroxycyclohex-2-en-1-ol (**2a**). The subsequent in situ synthesis of 2-bromocyclohexan-1,3-one (**II**) occurs through intermediate **I** upon reaction with NBS and Oxone. NBS provides bromine cations, which accelerate the formation of the α -monobrominated product (**II**), and the reaction requires oxygen in a stoichiometric ratio for this transformation to proceed.

The next step involves the addition of a urea derivative (**3a-f**) to the α -monobrominated product (**II**), producing intermediate **III**. Cyclization of intermediate **III** results in the formation of intermediate **IV**, driven by an intramolecular nucleophilic attack of the imine group on the carbonyl carbon. This cyclization leads to the final product (**4a-f**) following dehydration, as shown in **Scheme 3**.

In the next stage, 2-amino-5,5-dimethyl-5,6-dihydro-1,3-benzoxazol-7(4H)-one (**4a**) undergoes diazotization to form intermediate (**5a**), which reacts with ethyl acetoacetate in the presence of sodium acetate to yield ethyl-2-[(E)-(5,5-dimethyl-7-oxo-4,5,6,7-tetrahydro-1,3-benzoxazol-2-yl)diazenyl]-3-oxobutanoate (**6a**). This intermediate (**6a**) then undergoes a nucleophilic attack by hydrazine, which removes a water molecule. The pyrazolone ring closes as a result of an intramolecular nucleophilic attack, and the fused oxazole-linked pyrazole (**8a-f**) is formed through the loss of an alcohol molecule.



Scheme 3. Plausible mechanism for synthesis of fused oxazole (**4a-f**)



Scheme 4. Plausible mechanism for synthesis of pyrazolo-oxazole (**8a-f**)

2.4. Molecular Docking Studies

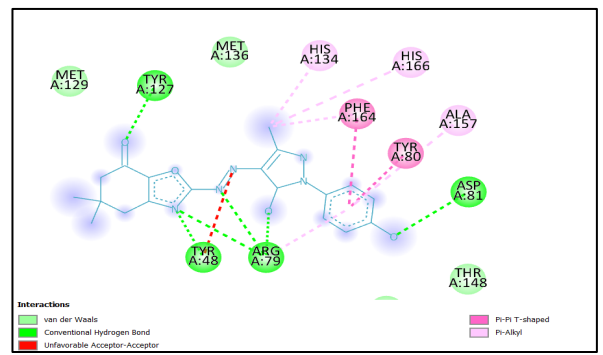
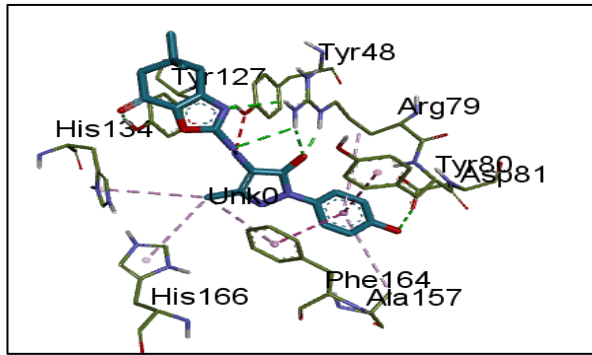
Visualization plays a crucial role in illustrating the structures and interactions of molecules, providing a better understanding of biomolecular relationships and the results of docking simulations. Docking is a valuable tool that reduces trial-and-error processes, saving time and resources. It efficiently filters large numbers of compounds and aids in ranking the most promising ones, especially when combined with visualization techniques. This combination enhances our understanding of disease pathophysiology and therapeutic processes. Proper interpretation and communication of docking simulation results require clear and educational visual representations.

BDS (Biomolecular Docking Software) offers a range of visualization tools for interpreting and communicating results. These tools include Ligand Explorer, which shows the interaction between proteins and ligands; Complex Viewer, which displays protein-ligand and protein-protein complexes; and the Electrostatic Potential Map, which represents the distribution of electrostatic potential on a protein's surface.

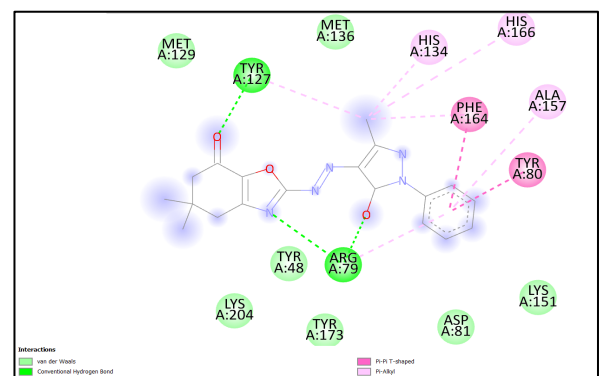
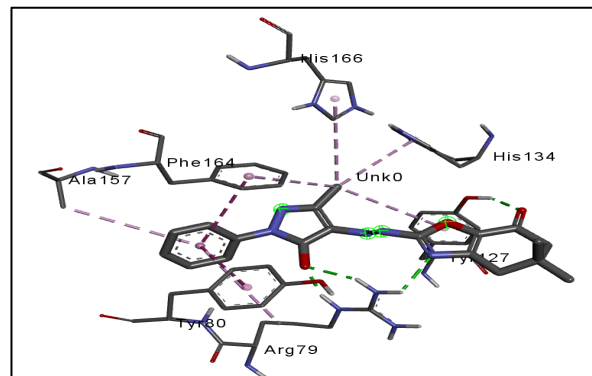
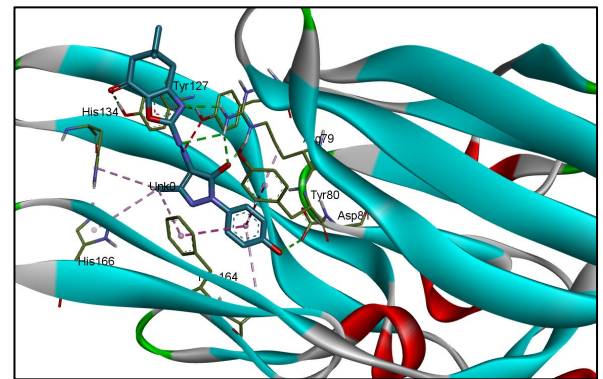
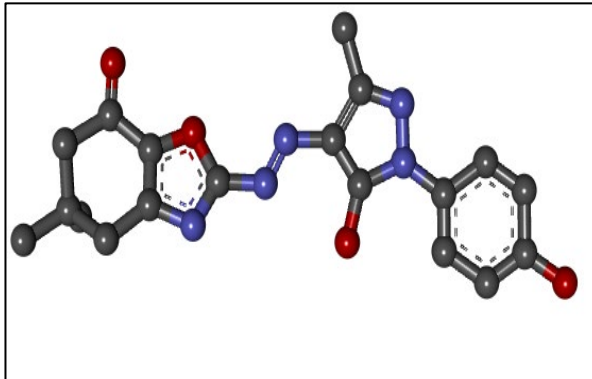
The goal of BDS's visualization tools is to help scientists understand and communicate the outcomes of molecular analyses, docking studies, and simulations. The approach emphasizes specific ligand-protein interactions, such as hydrophobic and hydrogen bonding, that influence complex stability and binding affinity. These tools provide guidance on how to effectively display molecular structures in three dimensions. BDS aims to integrate a variety of molecular modeling and simulation tools into a unified platform, offering comprehensive solutions for molecular biology research and drug development.

Table 5. Molecular docking scores of synthesized compounds (8a-f) versus heme-binding protein (PDB ID: 3H8T)

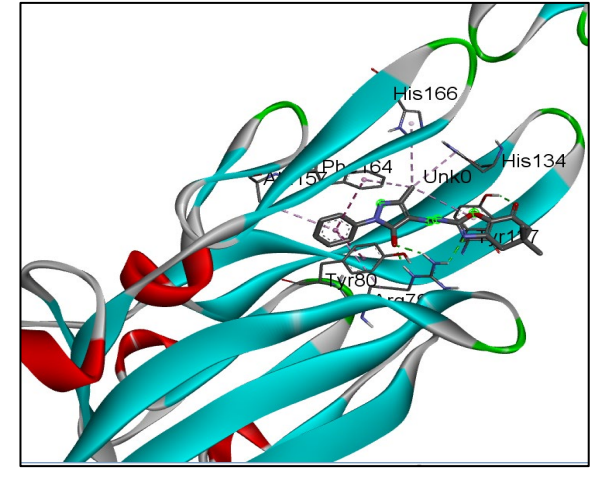
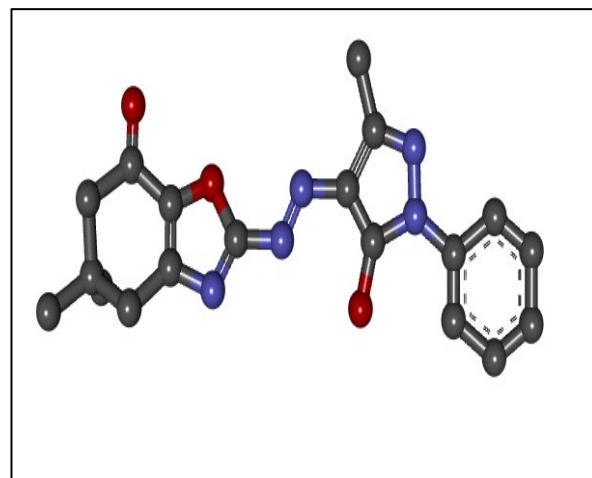
S. No.	Ligand- Protein 3D Interactions	
8a		
8b		

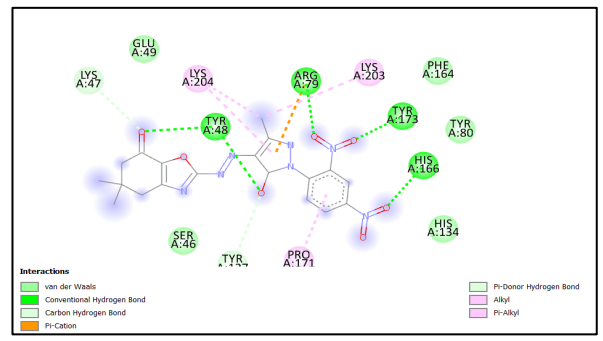
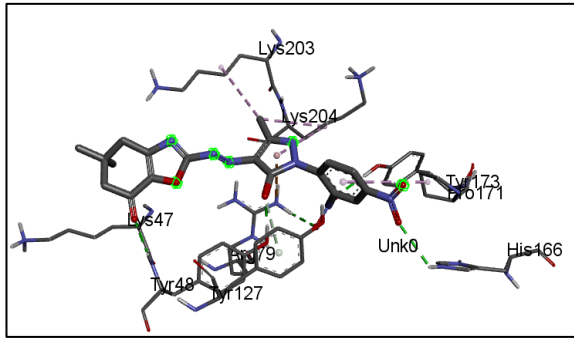


8c

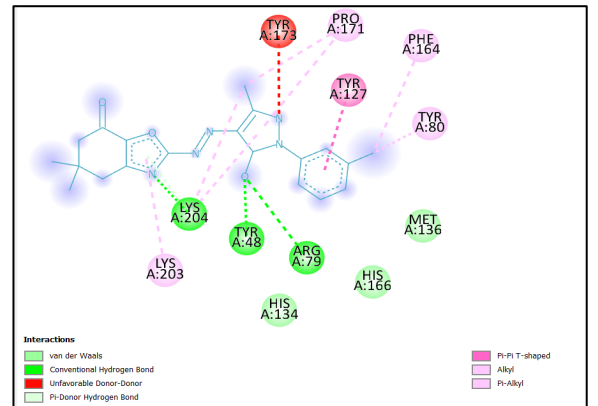
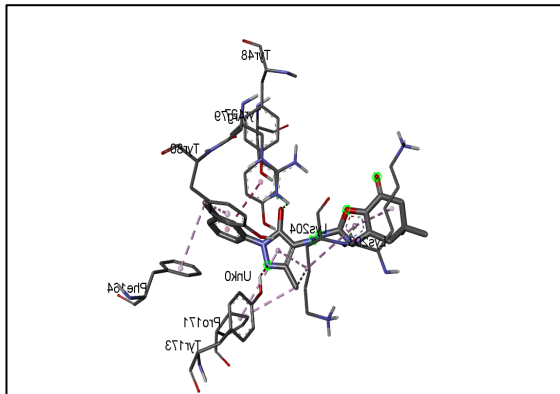
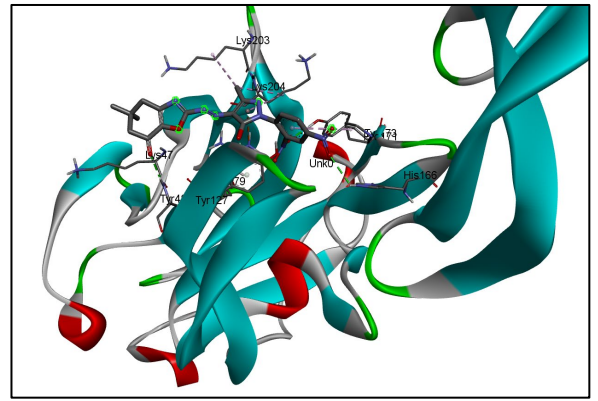
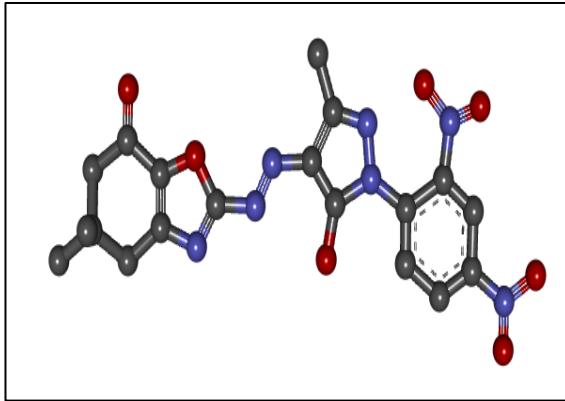


8d





8e



8f

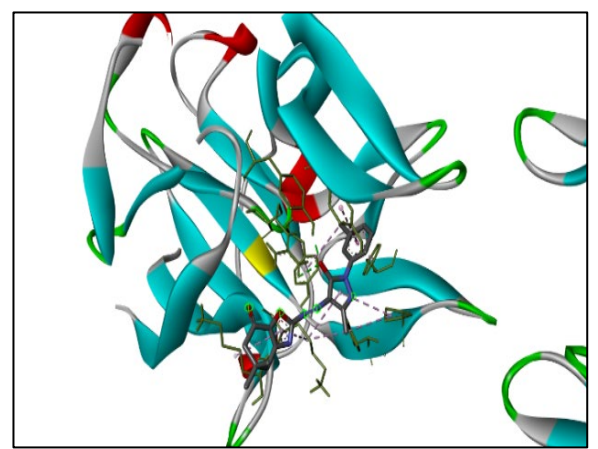
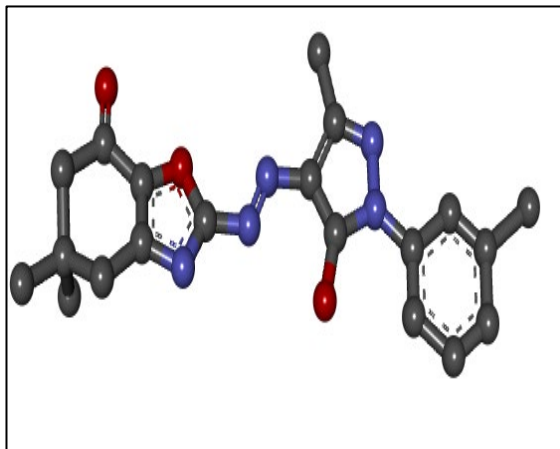


Table 6. Molecular docking studying of compounds (8a-f) against the target Heme binding protein (PDB ID: 3H8T)

S.No	Ligands	Docking Affinity (kcal/mol)	Hydrogen-Bond	Amino Acid Residual interaction		
				Hydrophobic/alkyl/ Pi-cation	Pi-Vander Waals	Vander Waals
1	8a	-10.0	His-166, His-134, Arg-79	Tyr-127, Phe-164, Tyr-80, Pro-171		Met-129, His-166, Lys-151, Thr-148
2	8b	-9.0	His-166, His-134, Arg-79	Pro-171, Tyr-80, Phe-164, Arg-79	Tyr-127	Met-129, Ala-169, Gly-170, Met-136, Asp-81, Lys-151, Thr-124
3	8c	-10.0	Arg-79, Tyr-127,	Arg-79, Ala-157, His-166, His-134	Tyr-127, Tyr-80, Phe-164	Lys-204, Tyr-173, Asp-81, Lys-151, Met-129, Met-136
4	8d	-9.5	Arg-79, Tyr-127	His-134, His-166, Phe-164, Ala-157, Tyr-80, Tyr-127		Met-129, Met-136, Lys-204, Tyr-173, Asp-81, Lys-151, Tyr-48
5	8e	-7.7	His-166, Tyr-173, Arg-79, Tyr-48, Lys-47, Tyr-127	Arg-79, Lys-203, Lys-204, Pro-171		Glu-49, Phe-164, Tyr-80, His-134, Ser-46
6	8f	-7.4	Lys-204, Tyr-48, Arg-79	Tyr-80, Phe-164, Lys-203, Tyr-127, pro-171, Tyr-173		Met-136, His-166, His-134,
7	Amoxicillin	-8.6	Tyr-173, Tyr-80, Arg-79, Arg-81	Pro-171		Thr-124, Tyr-48, Tyr-127, His-166, His-134, Met-129, His-78, Ala-157, Lys-151
8	Moxifloxacin	-8.6	Arg-122, Gln-154	Phe-164, Met-136, Pro-171, Lys-204, His-134		Tyr-80, His-166, Phe-156, Gly-155, Tyr-48, Thr-124
9	Sulfanilamide	-6	Tyr-48, Thr-124, Asp-81	Arg-79		His-78, Arg-122, Tyr-80, Lys-151
10	Sulfamethoxazole	-8.1	Thr-124, Tyr-48, Gly-155, Lys-151,	Leu-162, Phe-164, Ala-157, Tyr-80		Asp-81, Arg-122, Arg-79, Tyr-127

The six pyrazolo-oxazole compounds (8a–f), the heme binding protein, and their ligand–protein interactions are compared to conventional therapies for *P. gingivalis*. Compounds 8a, 8b, 8c, and 8d exhibit docking affinity scores of -10, -9, -10, and -9.5, respectively, compared to amoxicillin, moxifloxacin, sulfanilamide, and sulfamethoxazole, which have scores of -8.6, -8.6, -6, and -8.1.²⁵ Compounds 8e and 8f show higher docking scores than sulfanilamide but lower scores than the others (-7.7 and -7.4, respectively). Notably, compound 8e contains stronger hydrogen bonding interactions.

Table 5 shows that compounds 8e and 8f exhibit stable hydrogen bonds, along with weak hydrophobic and van der Waals interactions. The docking analyses of 8a–f suggest these compounds could serve as lead molecules for developing drugs with enhanced anticancer activities. However, further research is needed to address their toxicity and optimize dosages for treating diseases caused by *P. gingivalis*.

Studies on thiazole derivatives, quinazoline derivatives, and pyrrole-based drugs have shown similar docking affinity improvements over traditional antibiotics, indicating that heterocyclic scaffolds like pyrazolo-oxazoles have potential as antimicrobial agents. The pyrazolo-oxazole derivatives in this study demonstrate promising interactions with the heme binding protein of *P. gingivalis*, suggesting their potential for developing effective antimicrobial agents. Further validation studies are needed to confirm their efficacy and safety for clinical use.

3. Conclusion

This study presents a thorough investigation into the synthesis and potential pharmacological applications of pyrazolo-oxazole heterocyclic scaffolds using a solvent-free and additive-free approach. Molecular docking studies were conducted to explore the molecular interactions and biological activities of the synthesized compounds.

The findings indicate that the synthesized compounds exhibit promising interactions with the heme-binding protein associated with *P. gingivalis*, a bacterium implicated in various infections. Notably, compounds (8e) and (8f) demonstrate higher docking affinity scores compared to conventional medications, suggesting their potential as lead compounds for developing more effective pharmaceuticals against *P. gingivalis*-related diseases. Docking analyses reveal key molecular interactions influencing the binding affinities, including hydrophobic interactions, hydrogen bonding, and van der Waals forces. These insights open new avenues for optimizing these compounds to enhance their potency and reduce toxicity, ultimately contributing to the development of novel antimicrobial therapies.

Compounds (**8a–f**) exhibit significant potential as antimicrobial agents against *P. gingivalis*, with compounds (**8a**), (**8b**), (**8c**), and (**8d**) showing strong binding interactions. Compound (**8e**), despite having a slightly lower docking score, demonstrates more notable hydrogen bonding than any FDA-approved drug. These lead compounds hold promise for further structural optimization to enhance antimicrobial activity and therapeutic applications.

The development of efficient synthesis protocols and robust characterization methods underscores the significance of pyrazolo-oxazole derivatives in drug discovery. Further research focused on optimizing the compounds to reduce toxicity, determining appropriate dosing, and validating their clinical applications will be crucial for translating these findings into viable therapeutics for *P. gingivalis* infections and other bacterial diseases. This study provides a strong foundation for the development of new antimicrobial agents with improved efficacy and safety profiles.

4. Experimental

All chemicals were obtained from Sigma Aldrich and E. Merck, India, and used without further purification. Melting points were measured using a Veego melting-point apparatus, and all values are reported as observed. FT-IR spectra were recorded in the range of 400–4000 cm^{-1} using a Perkin-Elmer FTIR spectrometer. The ^1H NMR and ^{13}C NMR spectra were obtained using a Bruker Advance Neo 500-MHz NMR spectrometer (at 500 MHz) in CDCl_3 as the solvent. Chemical shifts are reported in ppm relative to tetramethylsilane (TMS). The splitting patterns observed were: s (singlet), d (doublet), t (triplet), dd (doublet of doublets), q (quartet), and m (multiplet).

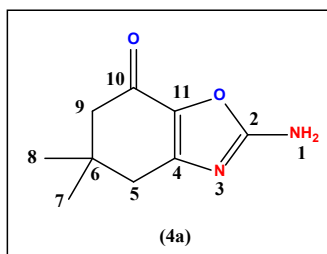
4.1. Procedure for the Preparation of Fused Oxazoles (**4a–f**)

Dimedone (1 mmol) and PTSA (0.5 mmol) were mixed in a 100 mL round-bottom flask. The reaction mixture was stirred for 10 minutes, after which NBS (1.3 mmol) was added dropwise. A light-yellow solution formed, turning golden yellow within 5 minutes. Oxone (1.2 mmol) was then added to the mixture, and magnetic stirring was continued at room temperature. The reaction progress was monitored by TLC using a 3:2 ethyl acetate and benzene solvent system. After 20 minutes, when the in-situ 2-bromocyclohexanone (**2**) was confirmed by TLC, the Urea derivatives (1 mmol, 1 equivalent) were added. The reaction mixture was stirred at 50°C , and TLC was again used to monitor progress. The reaction showed visible evolution over time. Once the reaction was complete, as indicated by TLC, the mixture was cooled and ethyl acetate (4×10 mL) was added. The organic layer was dried over sodium sulfate, filtered, and the desired product was isolated.

4.2. Synthesis of Fused Oxazole Linked with Pyrazole (**8a–f**)

To a solution of 2-amino-5,5-dimethyl-5,6-dihydro-1,3-benzoxazol-7(4H)-one (**4a**) (0.03 mol) in concentrated HCl (30 mL) and water (20 mL), sodium nitrite (0.03 mol) in 50 mL of water was added. The reaction mixture was cooled in an ice bath. Separately, a mixture containing ethyl acetoacetate (0.03 mol), sodium acetate (20 g), ethanol (15 mL), and water (50 mL) was prepared and cooled in an ice bath. The diazonium salt solution was slowly added to the second mixture while maintaining the temperature with the ice bath. The reaction mixture was stirred for 35 minutes, then filtered, washed with cold water, and recrystallized from ethanol. A mixture of the appropriate ethyl methyl [(5,5-dimethyl-7-oxo-4,5,6,7-tetrahydro-1,3-benzoxazol-2-yl)diazonyl]propanedioate (0.384 mmol) (**6a**) and hydrazine derivatives (**7a–f**) (0.37 mmol) was heated on a water bath for about 2 hours, with stirring using a glass rod. After the reaction, 50 mL of ether was added and the mixture was stirred vigorously for 15 minutes. A solid was observed to settle at the bottom of the flask. The residue was filtered, washed, and recrystallized from hot distilled water to obtain the desired product (**8a–f**).

4.3. The spectroanalytical data of the synthesized compounds **4(a–f)** and **8(a–f)** are as follows



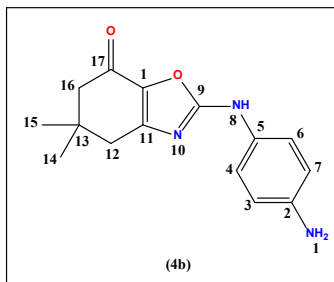
2-Amino-5,5-dimethyl-5,6-dihydro-1,3-benzoxazol-7(4H)-one (**4a**) was prepared using dimedone and urea as starting materials. Dark red solid; Yield: 92%; M.P.: $358\text{--}360^\circ\text{C}$;

FT-IR ($\bar{\nu}$ cm^{-1}): 3252 (N–H str.), 3024 (C–H sp^2), 2974 (C–H_{asym.} sp^3), 2942 (C–H_{sym.} sp^3), 1720 (C=O), 1628 (C=C/C=N), 1589, 1517, 1438 (C=C ring str.), 1120 (C–O) cm^{-1} ;

^1H NMR (500 MHz, DMSO): δ ppm 9.19 (s, 2H, NH₂), 6.34 (s, 2H, C-9), 6.09 (s, 2H, C-5), 1.11 (s, 6H, C-7, 8);

^{13}C NMR (125 MHz, CDCl₃): δ ppm 197.6 (C-10), 162.5 (C-2), 149.6 (C-11), 125.9 (C-4), 49.8 (C-9), 46.0 (C-5), 34.6 (C-6), 28.2 (C-7,8);

m/z : 180.07 [M+H]⁺; Anal. Cald. For C₉H₁₂N₂O₂: C, 59.99; H, 6.71; N, 15.55; O, 17.76 %. Found: C, 59.91; H, 6.75; N, 15.57; O, 17.78 %.



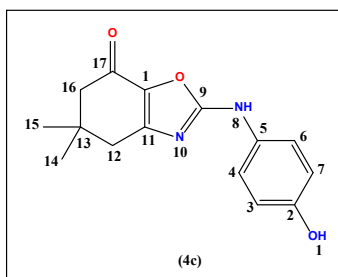
2-(4-Aminoanilino)-5,5-dimethyl-5,6-dihydro-1,3-benzoxazol-7(4H)-one (**4b**) was prepared using dimedone and 1-(4-aminophenyl) urea as starting materials. Light red solid; Yield: 87%; M.P.: 365-367 °C.

FT-IR ($\bar{\nu}$ cm⁻¹): 3259 (N-H str.), 3024 (C-H sp²), 2982 (C-Hasym. sp³), 2938 (C-H_{sym.} sp³), 1725 (C=O), 1631 (C=C/C=N), 1592, 1523, 1424 (C=C ring str.), 1123 (C-O) cm⁻¹;

^1H NMR (500 MHz, DMSO): δ ppm 10.94 (s, NH), 9.34 (s, 2H, NH₂), 7.44-7.42 (m, 2H, C-16), 7.13-7.12 (m, 2H, C-12), 6.42 (s, 2H, C-4,6), 6.12 (s, 2H, C-3,7), 1.19 (s, 6H, C-14,15);

^{13}C NMR (125 MHz, CDCl₃): δ ppm 178.47 (C-17), 161.63 (C-9), 144.99 (C-1), 143.78 (C-2), 131.64 (C-5), 129.91 (C-11), 129.75 (C-4), 129.68 (C-6), 117.54 (C-3), 117.23 (C-7), 114.15 (C-16), 113.52 (C-12), 113.31 (C-13), 39.25 (C-14,15);

m/z : 271.17 [M+H]⁺; Anal. Cald. For C₁₅H₁₇N₃O₂: C, 66.40; H, 6.32; N, 15.49; O, 17.79 %. Found: C, 66.36; H, 6.35; N, 15.47; O, 17.82 %.



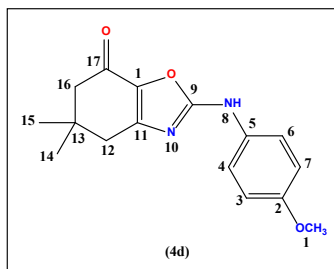
2-(4-Hydroxyanilino)-5,5-dimethyl-5,6-dihydro-1,3-benzoxazol-7(4H)-one (**4c**) was prepared using dimedone and 1-(4-hydroxyphenyl) urea as starting materials. Dark red solid; Yield: 86%; M.P.: 370-371 °C.

FT-IR ($\bar{\nu}$ cm⁻¹): 3560 (O-H str.), 3259 (N-H str.), 3026 (C-H sp²), 2993 (C-Hasym. sp³), 2916 (C-H_{sym.} sp³), 1722 (C=O), 1633 (C=C/C=N), 1596, 1519, 1416 (C=C ring str.), 1127 (C-O) cm⁻¹;

^1H NMR (500 MHz, DMSO): δ ppm 11.53 (s, OH), 10.89 (s, NH), 7.48-7.42 (m, 2H, C-16), 7.13-7.12 (m, 2H, C-12), 6.41 (s, 2H, C-4,6), 6.09 (s, 2H, C-3,7), 1.17 (s, 6H, C-14,15);

^{13}C NMR (125 MHz, CDCl₃): δ ppm 178.77 (C-17), 161.44 (C-9), 145.61 (C-1), 142.69 (C-2), 131.65 (C-5), 129.73 (C-11), 129.69 (C-4), 129.55 (C-6), 117.55 (C-3), 117.23 (C-7), 114.16 (C-16), 113.53 (C-12), 113.33 (C-13), 39.29 (C-14,15);

m/z : 272.07 [M+H]⁺; Anal. Cald. For C₁₅H₁₆N₂O₃: C, 66.16; H, 5.93; N, 10.29; O, 17.63 %. Found: C, 66.09; H, 5.95; N, 10.31; O, 17.68 %.



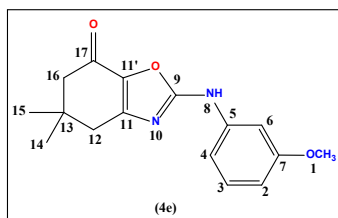
2-(4-Methoxyanilino)-5,5-dimethyl-5,6-dihydro-1,3-benzoxazol-7(4H)-one (**4d**) was prepared using dimedone and 1-(4-methoxyphenyl) urea as starting materials. Light red solid; Yield: 84%; M.P.: 361-362 °C.

FT-IR ($\bar{\nu}$ cm⁻¹): 3252 (N-H str.), 3029 (C-H sp²), 2986 (C-Hasym. sp³), 2903 (C-H_{sym.} sp³), 1728 (C=O), 1637 (C=C/C=N), 1588, 1523, 1405 (C≡C ring str.), 1119 (C-O) cm⁻¹;

¹H NMR (500 MHz, DMSO): δ ppm 10.78 (s, NH), 7.41-7.35 (m, 2H, C-16), 7.10-7.08 (m, 2H, C-12), 6.40 (s, 2H, C-4,6), 6.11 (s, 2H, C-3,7), 3.81 (s, 3H, C-1), 1.16 (s, 6H, C-14,15);

¹³C NMR (125 MHz, CDCl₃): δ ppm 178.55 (C-17), 160.64 (C-9), 143.60 (C-1), 143.44 (C-2), 130.64 (C-5), 129.91 (C-11), 129.75 (C-4), 129.68 (C-6), 117.55 (C-3), 117.23 (C-7), 114.05 (C-16), 113.52 (C-12), 113.30 (C-13), 39.05 (C-14,15);

m/z: 286.05 [M+H]⁺; Anal. Cald. For C₁₆H₁₈N₂O₃: C, 67.12.99; H, 6.34; N, 9.78; O, 16.76 %. Found: C, 67.10; H, 6.31; N, 9.80; O, 16.79 %.



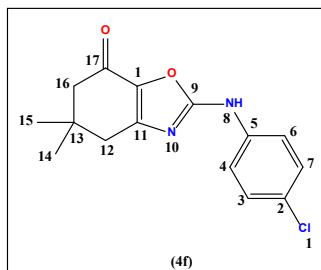
2-(3-Methoxyanilino)-5,5-dimethyl-5,6-dihydro-1,3-benzoxazol-7(4H)-one (**4e**) was prepared using dimedone and 1-(3-methoxyphenyl) urea as starting materials. Light red solid; Yield: 85%; M.P.: 373-376 °C.

FT-IR ($\bar{\nu}$ cm⁻¹): 3258 (N-H str.), 3018 (C-H sp²), 2991 (C-Hasym. sp³), 2914 (C-H_{sym.} sp³), 1734 (C=O), 1643 (C=C/C=N), 1593, 1532, 1418 (C≡C ring str.), 1124 (C-O) cm⁻¹;

¹H NMR (500 MHz, DMSO): δ ppm 10.69 (s, NH), 7.45-7.40 (m, 2H, C-16), 7.12-7.10 (m, 2H, C-12), 6.45 (s, 2H, C-3,4), 6.11 (s, 2H, C-2,6), 2.60 (s, 3H, C-1), 1.12 (s, 6H, C-14,15);

¹³C NMR (125 MHz, CDCl₃): δ ppm 178.43 (C-17), 161.47 (C-9, 11'), 145.64 (C-1), 143.68 (C-2), 131.46 (C-5), 129.77 (C-11), 129.54 (C-4), 129.51 (C-6), 117.54 (C-3), 117.20 (C-7), 114.15 (C-16), 113.52 (C-12), 113.31 (C-13), 39.23 (C-14,15);

m/z: 286.15 [M+H]⁺; Anal. Cald. For C₁₆H₁₈N₂O₃: C, 67.12.99; H, 6.34; N, 9.78; O, 16.76 %. Found: C, 67.09; H, 6.35; N, 9.79; O, 16.77 %.



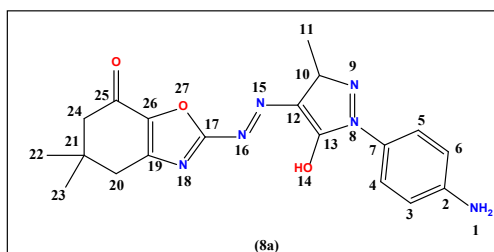
2-(4-Chloroanilino)-5,5-dimethyl-5,6-dihydro-1,3-benzoxazol-7(4H)-one (**4f**) was prepared using dimedone and 1-(4-chlorophenyl) urea as starting materials. Light red solid; Yield: 88% M.P.: 380-382 °C.

FT-IR ($\bar{\nu}$ cm^{-1}): 3253 (N-H str.), 3017 (C-H sp^2), 2994 (C-Hasym. sp^3), 2942 (C-H_{sym.} sp^3), 1718 (C=O), 1635 (C=C/C=N), 1587, 1518, 1429 (C=C ring str.), 1126 (C-O) cm^{-1} , 755 (C-Cl) cm^{-1} ;

^1H NMR (500 MHz, DMSO): δ ppm 10.89 (s, NH), 7.46-7.39 (m, 2H, C-16), 7.14-7.01 (m, 2H, C-12), 6.39 (s, 2H, C-4,6), 6.13 (s, 2H, C-3,7), 1.14 (s, 6H, C-14,15);

^{13}C NMR (125 MHz, CDCl_3): δ ppm 178.17 (C-17), 160.63 (C-9), 143.80 (C-1), 143.68 (C-2), 131.61 (C-5), 129.92 (C-11), 129.76 (C-4), 129.69 (C-6), 117.26 (C-3), 117.21 (C-7), 114.19 (C-16), 113.56 (C-12), 113.35 (C-13), 39.05 (C-14,15);

m/z : 290.71 $[\text{M}+\text{H}]^+$; Anal. Cald. For $\text{C}_{15}\text{H}_{15}\text{ClN}_2\text{O}_3$: C, 61.97; H, 5.20; Cl, 12.19; N, 9.64; O, 11.01 %. Found: C, 61.93; H, 5.22; Cl, 12.20; N, 9.61; O, 11.05 %.



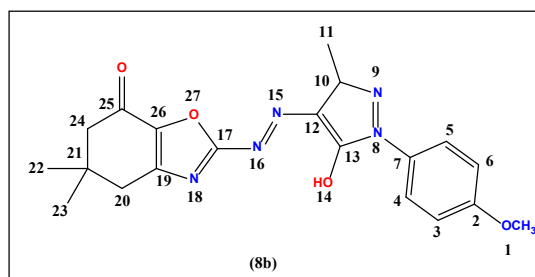
2-[(1E)-1-(4-Aminophenyl)-5-hydroxy-3-methyl-1H-pyrazol-4-ylazo]-5,5-dimethyl-1-oxa-3-aza-5,6-dihydroinden-7(4H)-one (**8a**) was prepared using 6a and 4-hydrazineylaniline as starting materials. Light red brown solid; Yield: 90%; M.P.: 383-384 $^{\circ}\text{C}$;

FT-IR ($\bar{\nu}$ cm^{-1}): 3463 (O-H str.), 3263 (N-H str.), 3029 (C-H sp^2), 2986 (C-Hasym. sp^3), 2934 (C-H_{sym.} sp^3), 1715 (C=O), 1593 (C=C/C=N), 1591, 1523, 1416 (C=C ring str.), 1127 (C-O) cm^{-1} ;

^1H NMR (500 MHz, DMSO): δ ppm 11.45 (s, OH), 7.39 (m, 2H, C-4,5), 6.59 (m, 2H, C-3,6), 6.24 (s, 2H, NH_2), 2.65 (s, 2H, C-20), 2.48 (s, 2H, C-24), 2.37 (s, 3H, C-11), 0.99 (s, 6H, C-22,23);

^{13}C NMR (125 MHz, CDCl_3): δ ppm 177.33 (C-25), 163.66 (C-13), 144.98 (C-17), 143.79 (C-26), 143.65 (C-2), 130.66 (C-7), 129.90 (C-19), 129.67 (C-12), 129.15 (C-4, 5), 117.58 (C-3,6), 117.28 (C-10), 114.88 (C-24), 113.53 (C-20), 113.29 (C-21), 39.06 (C-22,23), 28.28 (C-11);

m/z : 380.03 $[\text{M}+\text{H}]^+$; Anal. Cald. For $\text{C}_{19}\text{H}_{20}\text{N}_6\text{O}_3$: C, 59.99; H, 5.30; N, 22.09; O, 12.62 %. Found: C, 59.91; H, 5.34; N, 22.11; O, 12.64 %.



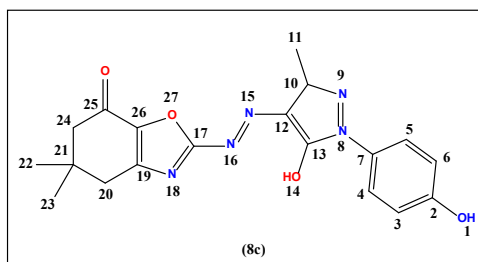
2-[(1E)-5-Hydroxy-1-(4-methoxyphenyl)-3-methyl-1H-pyrazol-4-ylazo]-5,5-dimethyl-1-oxa-3-aza-5,6-dihydroinden-7(4H)-one (**8b**) was prepared using 6a and 4-methoxy phenyl hydrazine as starting materials. Brown solid; Yield: 87%; M.P.: 383-386 $^{\circ}\text{C}$;

FT-IR ($\bar{\nu}$ cm^{-1}): 3495 (O-H str.), 3257 (N-H str.), 3034 (C-H sp^2), 2995 (C-Hasym. sp^3), 2926 (C-H_{sym.} sp^3), 1719 (C=O), 1587 (C=C/C=N), 1593, 1518, 1409 (C=C ring str.), 1131 (C-O) cm^{-1} ;

^1H NMR (500 MHz, DMSO): δ ppm 11.41 (s, 1H, OH), 7.37 (m, 2H, C-4,5), 6.57 (m, 2H, C-3,6), 3.81 (s, 3H, C-1), 2.62 (s, 2H, C-20), 2.49 (s, 2H, C-24), 2.37 (s, 3H, C-11), 0.99 (s, 6H, C-22,23);

^{13}C NMR (125 MHz, CDCl_3): δ ppm 177.40 (C-25), 161.60 (C-13), 144.89 (C-17), 143.77 (C-26), 143.61 (C-2), 131.64 (C-7), 129.96 (C-19), 129.69 (C-12), 129.09 (C-4, 5), 117.58 (C-3,6), 117.29 (C-10), 114.78 (C-24), 113.58 (C-20), 113.21 (C-21), 55.83 (C-1), 39.27 (C-22,23), 28.27 (C-11);

m/z : 395.11 $[M+H]^+$; Anal. Cald. For $C_{20}H_{21}N_5O_4$: C, 60.75; H, 5.30535; N, 17.71; O, 16.19 %. Found: C, 60.71; H, 5.33; N, 17.75; O, 16.21 %.



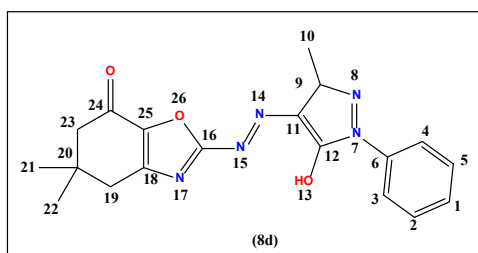
2-[(1E)-1-(4-Hydroxyphenyl)-5-hydroxy-3-methyl-1H-pyrazol-4-ylazo]-5,5-dimethyl-1-oxa-3-aza-5,6-dihydroindeno-7(4H)-one (**8c**) was prepared using **6a** and 4-hydroxy phenyl hydrazine as starting materials. Light brown solid; Yield: 86%; M.P.: 375-377 °C;

FT-IR ($\bar{\nu}$ cm^{-1}): 3498 (O-H str.), 3253 (N-H str.), 3028 (C-H sp^2), 2989 (C-Hasym. sp^3), 2919 (C- $H_{sym.}$ sp^3), 1724 (C=O), 1587 (C=C/C=N), 1593, 1518, 1409 (C=C=C ring str.), 1131 (C-O) cm^{-1} ;

1H NMR (500 MHz, DMSO): δ ppm 11.46 (s, 1H, OH), 7.33 (m, 2H, C-4,5), 6.59 (m, 2H, C-3,6), 5.35 (s, 1H, OH-1), 2.68 (s, 2H, C-20), 2.49 (s, 2H, C-24), 2.39 (s, 3H, C-11), 0.99 (s, 6H, C-22,23);

^{13}C NMR (125 MHz, $CDCl_3$): δ ppm 177.30 (C-25), 163.60 (C-13), 144.99 (C-17), 143.78 (C-26), 143.64 (C-2), 143.44 (C-7), 130.64 (C-19), 129.75 (C-12), 119.21 (C-4,5), 117.59 (C-3,6), 117.25 (C-10), 114.99 (C-24), 113.52 (C-20), 113.29 (C-21), 39.26 (C-22,23), 28.90 (C-11);

m/z : 381.24 $[M+H]^+$; Anal. Cald. For $C_{19}H_{19}N_5O_4$: C, 59.84; H, 5.02; N, 18.36; O, 16.78 %. Found: C, 59.79; H, 5.04; N, 18.38; O, 16.79 %.



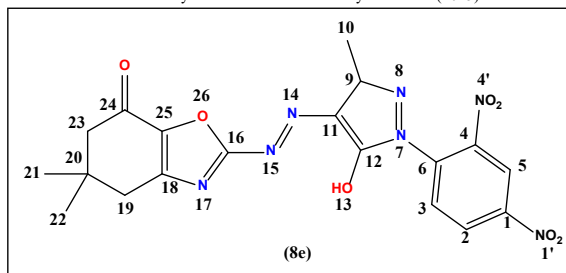
2-[(1E)-5-Hydroxy-3-methyl-1-(phenyl)-1H-pyrazol-4-ylazo]-5,5-dimethyl-1-oxa-3-aza-5,6-dihydroindeno-7(4H)-one (**8d**) was prepared using **6a** and phenyl hydrazine as starting materials. Light red black solid; Yield: 84%; M.P.: 389-390 °C;

FT-IR ($\bar{\nu}$ cm^{-1}): 3485 (O-H str.), 3261 (N-H str.), 3026 (C-H sp^2), 2992 (C-Hasym. sp^3), 2921 (C- $H_{sym.}$ sp^3), 1731 (C=O), 1579 (C=C/C=N), 1588, 1523, 1412 (C=C=C ring str.), 1127 (C-O) cm^{-1} ;

1H NMR (500 MHz, DMSO): δ ppm 12.40 (s, 1H, OH), 7.42-7.24 (m, 3H, C-1, 2, 5), 7.22-7.14 (m, 2H, C-3,4), 7.12 (s, 2H, C-19), 7.05-6.84 (s, 2H, C-23), 2.59 (s, 6H, C-21,22), 2.42 (s, 3H, C-10);

^{13}C NMR (125 MHz, $CDCl_3$): δ ppm 177.31 (C-24), 163.60 (C-12), 144.91 (C-16), 143.75 (C-25), 143.40 (C-6), 130.64 (C-18), 129.77 (C-11), 129.52 (C-3,4), 129.44 (C-2,5), 129.29 (C-1), 117.25 (C-9), 114.99 (C-23), 113.50 (C-19), 113.22 (C-20), 39.26 (C-21,22), 28.90 (C-10);

m/z : 365.09 $[M+H]^+$; Anal. Cald. For $C_{19}H_{20}N_6O_3$: C, 62.46; H, 5.2; N, 19.17; O, 13.14 %. Found: C, 62.49; H, 5.29; N, 19.13; O, 13.10 %.



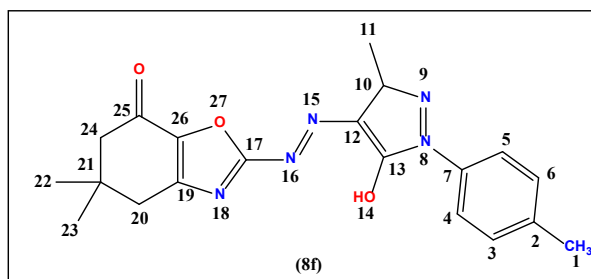
2-[(1E)-5-Hydroxy-3-methyl-1-(2,4-dinitrophenyl)-1H-pyrazol-4-ylazo]-5,5-dimethyl-1-oxa-3-aza-5,6-dihydroindeno-7(4H)-one (**8e**) was prepared using 6a and 2,4-dinitrophenyl hydrazine as starting materials. Dark brown solid; Yield: 85%; M.P.: 373-374 °C.

FT-IR ($\bar{\nu}$ cm⁻¹): 3488 (O-H str.), 3257 (N-H str.), 3032 (C-H sp²), 2989 (C-Hasym. sp³), 2918 (C-Hsym. sp³), 1726 (C=O), 1583 (C=C/C=N), 1592, 1516, 1408 (C≡C ring str.), 1528 (NO₂asym.), 1342 (NO₂sym.), 1133 (C-O) cm⁻¹;

¹H NMR (500 MHz, DMSO): δ ppm 12.48 (s, 1H, OH), 7.62 (s, 1H, C-5), 7.52-7.03 (m, 2H, C-2,3), 6.23 (s, 2H, C-19), 6.10 (s, 2H, C-23), 2.57 (s, 6H, C-21,22), 2.41 (s, 3H, C-10);

¹³C NMR (125 MHz, CDCl₃): δ ppm 178.25 (C-24), 163.65 (C-12), 144.99 (C-6), 143.77 (C-16), 143.64 (C-25), 143.51 (C-1), 130.29 (C-4), 129.78 (C-2), 129.65 (C-18), 129.44 (C-3), 129.05 (C-14), 117.63 (C-5), 117.25 (C-9), 114.92 (C-23), 113.90 (C-19), 113.54 (C-20), 39.27 (C-21,22), 28.76 (C-10);

m/z: 455.16 [M+H]⁺; Anal. Cald. For C₁₉H₁₇N₇O₇: C, 50.11; H, 3.76; N, 21.53; O, 24.59 %. Found: C, 50.15; H, 3.73; N, 21.49; O, 24.62 %.



2-[(1E)-5-Hydroxy-1-(4-methylphenyl)-3-methyl-1H-pyrazol-4-ylazo]-5,5-dimethyl-1-oxa-3-aza-5,6-dihydroindeno-7(4H)-one (**8f**) was prepared using 6a and 4-methyl phenyl hydrazine as starting materials. Light brown solid; Yield: 88%; M.P.: 369-370 °C;

FT-IR ($\bar{\nu}$ cm⁻¹): 3491 (O-H str.), 3264 (N-H str.), 3028 (C-H sp²), 2992 (C-Hasym. sp³), 2923 (C-H_{sym.} sp³), 1731 (C=O), 1577 (C=C/C=N), 1586, 1524, 1415 (C≡C ring str.), 1124 (C-O) cm⁻¹;

¹H NMR (500 MHz, DMSO): δ ppm 12.39 (s, 1H, OH), 7.85 (m, 2H, C-4,5), 7.51 (m, 2H, C-3,6), 6.22 (s, 2H, C-20), 6.10 (s, 2H, C-24), 2.57 (s, 6H, C-22,23), 2.37 (s, 3H, C-11), 2.34 (s, 3H, C-1);

¹³C NMR (125 MHz, CDCl₃): δ ppm 177.39 (C-25), 162.60 (C-13), 143.99 (C-17), 143.78 (C-26), 143.63 (C-2), 130.61 (C-7), 129.89 (C-19), 129.61 (C-12), 129.25 (C-4, 5), 117.59 (C-3,6), 117.28 (C-10), 114.87 (C-24), 113.55 (C-20), 113.26 (C-21), 39.27 (C-22,23), 28.26 (C-11), 21.83 (C-1);

m/z: 379.02 [M+H]⁺; Anal. Cald. For C₂₀H₂₁N₅O₃: C, 63.31; H, 5.58; N, 18.46; O, 12.65 %. Found: C, 63.27; H, 5.61; N, 18.43; O, 12.69 %.

Acknowledgments

The authors would like to thank the Director, SAIF, Punjab University, Chandigarh, for providing the spectroanalytical data and results. They also thank the Head, School of Chemical Sciences, Devi Ahilya Vishwavidyalaya, Indore for providing all the necessary research facilities.

References

1. Tietze L., Rackelmann N. (2004) Domino reactions in the synthesis of heterocyclic natural products and analogs. *Pure Appl. Chem.*, 76(11) 1967-1983.
2. Ankodia V., Sharma P., Sharma K., Kumar M., Gupta A. (2009) Regioselective OnePot Synthesis of 5-Chloro-3-methyl-8-trifluoromethyl-4H-1,4-benzothiazines. *Heterocycl. Commun.*, 15(2) 127-134.
3. Ankodia, V., Sharma P.K., Gupta V., Kumar M. (2008) Synthesis of 2, 4-diaryl-2, 3-dihydro-1, 5-benzothiazepines. *Heterocycl. Commun.*, 14(3) 155-160.
4. Zhang B., Studer A. (2015) Recent advances in the synthesis of nitrogen heterocycles via radical cascade reactions using isonitriles as radical acceptors. *Chem. Soc. Rev.*, 44(11) 3505-3521.
5. Kel'in A.V., Sromek A.W., Gevorgyan V. (2001) A novel Cu-assisted cycloisomerization of alkynyl imines: Efficient synthesis of pyrroles and pyrrole-containing heterocycles. *J. Am. Chem. Soc.*, 123(9), 2074-2075.
6. Mahmood R.M.U., Aljamali N.M. (2020) Synthesis, spectral investigation, and microbial studying of pyridine-heterocyclic compounds. *Eur. J. Mol. Clin. Med.*, 7, 4444-4453.
7. Midya S.P., Landge V.G., Sahoo M.K., Rana J., Balaraman E. (2017) Cobalt-catalyzed acceptorless dehydrogenative coupling of aminoalcohols with alcohols: Direct access to pyrrole, pyridine and pyrazine derivatives. *Chem. Commun.*, 54(1), 90-93.
8. Alvarez-Builla J., Barluenga J. (2011) Heterocyclic compounds: An introduction. *Mod. Heterocycl. Chem*, 1, 1-9.
9. Chaucer P., Sharma P.K. (2020) Study of thiazines as potential anticancer agents. *Plant Arch.*, 20, 3199-3202.
10. Zhang H., Liu C. (2017) Synthesis and properties of furan/thiophene substituted difluoroboron β -diketonate derivatives bearing a triphenylamine moiety. *Dyes Pigm.*, 143, 143-150.
11. Raychev D., Guskova O., Seifert G., Sommer J.U. Conformational and electronic properties of small benzothiadiazole-cored oligomers with aryl flanking units: Thiophene versus furan. *Comput. Mater. Sci.*, 126, 287-298.
12. Hossain M., Nanda A.K. (2018) A review on heterocyclic: Synthesis and their application in medicinal chemistry of imidazole moiety. *Sci. J. Chem.*, 6, 83-94.
13. Jampilek J. (2019) Heterocycles in medicinal chemistry. *Mol.* 24(21), 3839.
14. Ji Y., Fan Y., Liu K., Kong D., Lu J. (2015) Thermo activated persulfate oxidation of antibiotic sulfamethoxazole and structurally related compounds. *Water Res.*, 87, 1-9.
15. Panchal N.B., Patel P.H., Chhipa N.M., Parmar R.S. (2020) Acridine a versatile heterocyclic moiety as anticancer agent. *Int. J. Pharm. Sci. Res.*, 11, 4739-4748.
16. Marín-Ocampo L., Veloza L.A., Abonia R., Sepúlveda-Arias J.C. (2019) Anti-inflammatory activity of triazine derivatives: A systematic review. *Eur. J. Med. Chem.*, 162, 435-447.
17. Campanati M., Vaccari A., Piccolo O. (2000) Environment-friendly synthesis of nitrogen-containing heterocyclic compounds. *Catal. Today*, 60(3-4), 289-295.
18. Vekariya R.H., Patel K.D., Prajapati N.P., Patel H.D. (2018) Phenacyl bromide: A versatile organic intermediate for the synthesis of heterocyclic compounds. *Synth. Commun.*, 48(13), 1505-1533.
19. Ye Z., Zhang F. (2019) Recent advances in constructing nitrogen-containing heterocycles via electrochemical dehydrogenation. *Chin. J. Chem.*, 37(5), 513-528.
20. Lelyukh, M. I., Komarenska, Z. M., Chaban, T. I., Chaban, I. H. (2024) An overview of the synthetic routes toward [1,2,4]triazolo[3,4-b][1,3,4]thiadiazoles (microreview). *Chem. Heterocycl. Comp.*, 60(7), 342-344.
21. Prakash, C., Singh, R. (2024) Synthesis of fluorinated six-membered nitrogen heterocycles using microwave irradiation. *Chem. Heterocycl. Comp.*, 60(5), 216-229.
22. Zhilitskaya, L. V., Yarosh, N. O. (2024) The synthesis of salts of five-membered heterocyclic compounds based on N-containing cations/anions (microreview). *Chem. Heterocycl. Comp.*, 60(5), 230-232.
23. Chaban, T. I., Klenina, O. V., Chaban, I. H., Lelyukh, M. I. (2024) Recent advances in the synthesis of thiazolo[4,5-b]pyridines. part 2: focus on thiazole annulation to pyridine ring. *Chem. Heterocycl. Comp.*, 60(3-4), 130-132.
24. Zheng X., Liu W., Zhang D. (2020) Recent Advances in the Synthesis of Oxazole-Based Molecules via van Leusen Oxazole Synthesis. *Mol.*, 25(7), 1594.
25. Manikandan P., Veeraraghavan V. P., Sekaran S., Rengasamy G., Eswaramoorthy R. (2023) Molecular docking analysis of oxazole compounds with the heme-binding protein from *Porphyromonas gingivalis*. *Bioinform.*, 19(1), 105-110.
26. Daswani U., Dubey N., Sharma P., Kumar A. (2016) A new NBS/Oxone promoted one pot cascade synthesis of 2-aminobenzimidazoles/2-aminobenzoxazoles: a facile approach. *New J. Chem.*, 40(9), 8093-8099.

